Mixed, quantum-classical description of electron density transfer in the collision process

Paweł Wojda[a], Marta Łabuda[b,c] and Sergey Kshevetskii[d]

[a]Institute of Applied Mathematics, Faculty of Applied Physics and Mathematics, Gdańsk University of Technology, Gdańsk, Poland; [b]Institute of Physics and Applied Computer Science, Faculty of Applied Physics and Mathematics, Gdańsk University of Technology, Gdańsk, Poland; [c]BioTechMed Center, Gdańsk University of Technology, Gdańsk, Poland; [d]Physics Department, Immanuel Kant Baltic Federal University, Kaliningrad, Russia

ARTICLE HISTORY
Compiled June 14, 2024

Abstract
In this work, we investigate an ion-atom model describing the time-dependent evolution of electron density during the collision. For a $S^{3+} - H$ system, numerical simulations are based on classical trajectory calculations, and the electron density behaviour is described with the time-dependent Schrödinger equation. We apply the finite difference method to obtain quantitative insights into the charge transfer dynamics, providing detailed information about the spatial and temporal evolution of the collision process. The results are given for representative examples of the collision, from eV to keV range of energies, in head-on collision as well as for different values of impact parameter. A validity and precision of the proposed model and interpretation of the particle collision in terms of eigenstates are also discussed.

KEYWORDS
Electron density transfer; dynamics of ions interaction; finite difference method; Schrödinger equation

1. Introduction

From a molecular point of view, during the study of ion-atom collision reactions, the electrons can be shared by both the target and projectile, forming a quasi-molecule $(AB)^{q+}$ by which the evolution of the collision system in a molecular framework may be represented. In the standard approach, the Born-Oppenheimer approximation is used to solve the Schrödinger equation, which allows that the nuclei are fixed with respect to the motion of the electrons. The solution of the Schrödinger equation, taking account of the separation of the nuclear and electronic motions, leads to a set of coupled equations for the determination of the nuclear functions, from the knowledge of the electronic functions. The eigenfunctions of the ground and several first excited states of the collision system calculated within the Hartree-Fock method, are used as the system of orthogonal basis electronic functions. The electronic basis functions under consideration parametrically depend on the distance R between the particles forming the system which varies in time t during the collision, therefore, the functions

CONTACT P. Wojda. Email: pawwojda@pg.edu.pl

depend on time as well. The time-dependence of basis functions is usually not taken into account. Based on the non-stationary Schrödinger equation, one derives the differential equations in time for a series of coefficients. When these differential equations are solved, an approximate description of the dynamics of the system is achieved. The comparison between calculated results with the experimental data shows that such an approach adequately describes the particle collision. Nevertheless, it is not explicitly possible to control the accuracy of the obtained approximate solution with mathematical means. In ion-atom collisions, both, the electronic structure of the target and the behaviour of the projectile ion play a significant role. From a theoretical point of view, the description of the charge transfer (CT) in collisions between accelerated heavy ions and neutral atoms has been widely investigated in the literature [1], [2], [3]. The importance of this process is evident in different fields of science such as chemistry, material science, astrophysics, laser research, biophysics, and others [4], [5], [6], [7], [8], [9], [10].

In the keV energy range, a commonly used approach is the resolution of the stationary close-coupling equations ([11] and references therein, [12]). However, in the low-energy range of a few eV, the number of theoretical studies dealing with atomic or ionic collisions is quite limited due to the need of a specific treatment of the collision dynamics with regard to the energy range. In practice, the quantum chemical calculations of the transfer of an electron between two particles (atoms, ions, molecules, etc.) requires: i) the correct description of the electronic structure of the collisional partners and, ii) the employment of an appropriate method that is able to account for the dynamics of the collision. In particular, when the energy of the incident particles is in the range of a few eV, an exact quantum-mechanical description of the dynamics of both the electrons and the nuclei is required [11], [13], [14], [15]. Such a description can be, in principle, obtained by following the wave function by means of the time-dependent Schrödinger equation (TDSE). It is known that the main interest of the wave packet method over the time-independent close-coupling approach appears clearly in polyatomic systems, since there exists the possibility of developing a fully quantum mechanical treatment for some degrees of freedom while others behave classically. It has been known that the use of classical or semiclassical approximations can provide, to a certain extent, reasonable descriptions of the dynamics of nuclei in a polyatomic system. This is the basis of the so-called quasiclassical trajectory (QCT) approach also known as the adiabatic molecular-dynamics (AMD) method [16]. The semiclassical coupled wave-packet approach that treats electronic and vibrational (whether bound or dissociative) motions quantally and the remaining motions classically is also one of the most developed theories, applied in example in the investigation of the dynamics of fragmentation of Na_2^+ dimer ions with the keV He atom [17]. However, this method is computationally quite demanding, especially in the low collision energy range.

The efficiency and numerical stability of time-dependent wave packet methods applied on ion-atom collisions has been discussed widely in many exemplary publications such as: [18], [19], [20], [21]. Therefore, also the development of time-dependent theories was implemented using a small (but from a computational point of view attractive) model of S^{3+} and H collision. This simple case served as an illustration of the nuclear and electron motions over time. In particular, the quantum wave packet calculations have been carried out in one (1D) and two (2D) dimensions [22], [23] for the kinetic energies of the projectile between 1-10 eV. The evolution of the wave packet in the femtosecond (1 fs=10^{-15} s) time scale as well as—for the first time—the CT reaction via time-dependent electronic density $\varrho(r,t)$ has been presented. The evolution of the

global electronic density in the three-dimensional (3D) grid for all the states taking part in the $S^{3+}+H$ process was visualized by the snapshots of the simulation movie [23]. Additionally, an angular distribution of the scattered wave packet and the final probability of electron exchange vs. initial kinetic energy of the projectile have also been calculated.

On the other hand, a theoretical framework that combines elements of both classical and quantum mechanics to describe the behavior of a system can be also used. Application of such a mixed, quantum-classical approach is particularly useful when dealing with complex systems, where a fully quantum mechanical treatment may be computationally expensive or impractical [24]. Such a hybrid description involves employing quantum mechanics to model the initial and final states of electrons, while employing classical mechanics to track the intermediate stages of their trajectories during the collision. Particularly, more recently developed mixed quantum/classical theory of inelastic scattering (MQCT) approach became very efficient [25], [26], [27] in which quantum state-to-state transitions between the internal states of the molecule are described using a TDSE, while the scattering of collision partners is described classically using mean-field trajectories. Initiated by the work of [28] and fully quantal treatment of radiative charge transfer for diatomics, i.e. by Stancil et al.[29], [30] and more recently developed by the group of Babikov et al. [27], [31] this method become an interesting solution for studying energy transfer during collision for a broad range of collision energies.

In this work, the collision system is represented by the ion-atom interaction of $S^{3+} + H$. Electron configuration of positively charged ion S^{3+} depends on its specific charge state and it involves the removal of electrons from the valence shells of a neutral sulfur atom. The hydrogen atom $H(1s)$ has one electron in the neutral state. By examining the electronic structure of the interacting particles, we gain insight into the distribution of electrons before and after the collision, laying the foundation for understanding the transfer dynamics. The present study is also based on the mean-field Ehrenfest method (see [32], [33]), which is equivalent to the Ehrenfest approach, where the average of potential over the electronic wavefunction is used to propagate the equations of motion for the nuclei. In this case, the average is computed over the quantum wave function defined on a grid, rather than over a set of eigenstates.

Here, to solve the TDSE the finite-difference method (FDM) is applied. FDM provides numerical solutions to the differential equations governing the collision dynamics and is computationally efficient [34], [35]. In order to investigate the collision process and, in particular, the electron density transfer during a collision, we based on the numerical scenario proposed by [36]. To check the validity and efficiency of the method, we performed the calculations for different values of the collision energy, such as $E = 13$ eV, $E = 325$ eV as well as $E = 5$ keV in the head-on collision of the interaction. The impact parameter approximation which plays an important role in the investigation of the collision products has been also utilized. Indeed, the collision between S^{3+} and hydrogen (H) with a specified impact parameter involves studying the interaction between the particles as they approach each other with a certain relative velocity and miss each other by a specified distance. Therefore, several impact parameters between $b \in [0, 5]$ a.u. have been tested in the model numerical simulations. They reveal scattering patterns of electron density transfer, exhibiting regions of high probability density as electrons travel across from the ion to the atom. Indeed, the interplay between repulsive and attractive forces during the collision significantly influences the outcome, dictating whether electron density is captured or repelled. Moreover, based on the collision energy for the system of $S^{3+} - H$, an analysis of the results was carried out

in terms of eigenstates to asses whether the collision will lead to the transfer of an electron from hydrogen to the sulfur ion (the transfer is highly probable) or whether the electron will remain in the vicinity of hydrogen.

2. Particle system Hamiltonian. Mixed, quantum-classical description of dynamics

In our treatment, a H atom is interpreted as a proton and an electron interacting with it, and with the sulfur ion of $+3e$ which are interacting in agreement with Coulomb's law. In the performed simulations, the valence electrons of the S ion are not taken into account separately and the pseudopotentials are not applied to describe the electric field of the S^{3+}. A S^{3+} model may seem overly simplified, but the performed simulations show that in the slow, eV collision energy range, the ions do not approach each other, which is why the potential of the ion at such distances follows the shape of the Coulomb one. Below, important model details are presented.

The Hamiltonian of the system we are considering, consisting of one electron and two ions, has the form:

$$\hat{H} = \hat{H}_E + \hat{H}_I \tag{1}$$

where

$$\hat{H}_E = \left(-\frac{\hbar^2}{2m_e}\Delta\right) - \sum_J \frac{Z_J e^2}{\left|\overrightarrow{r} - \overrightarrow{R}_J\right|} = \left(-\frac{\hbar^2}{2m_e}\Delta + U\right) \tag{2}$$

$$\hat{H}_I = \sum_J \frac{p_J^2}{2m_J} + \frac{Z_1\, Z_2\, e^2}{\left|\overrightarrow{R}_2 - \overrightarrow{R}_1\right|} \tag{3}$$

In expression (1), $\sum_J$ is a sum of two nuclei; Z_J is the charge of the nucleus with number J, expressed in charges $|e|$ of an electron; $\overrightarrow{R}_J$ is a position of the nucleus J; $\overrightarrow{r}$ is a radius-vector for the electron; and p_J and m_J are the momentum and mass of the nucleus with number J, respectively. The evolution of the particle system is described as follows. We assume that the motion of ions can be described by the classical mechanics equations (since the values of the ion masses are relatively large), and the ion energies are not small enough that quantum effects noticeably affect the ions' movement:

$$\begin{array}{c} \frac{d\vec{R}_J}{dt} = \frac{\partial H_{classic}}{\partial \vec{p}_J} \\ \frac{d\vec{p}_J}{dt} = -\frac{\partial H_{classic}}{\partial \vec{R}_J} \end{array}, \tag{4}$$

$$H_{classic} = \frac{p_e^2}{2m_e} + U_{classic} + \sum_J \frac{p_J^2}{2m_J} + \frac{Z_1\, Z_2\, e^2}{\left|\overrightarrow{R}_2 - \overrightarrow{R}_1\right|} \tag{5}$$

where $\overrightarrow{R}_J$ is the position, and $\overrightarrow{p}_j$ is the momentum of the ion with the number J. In formula (4), the potential $U_{classic}$ of the interaction of the ions with an electron is described as the quantum mechanical average: $U_{classic} = \langle \Psi \,|\, U\Psi \rangle$, where Ψ is

an electron wave function defined below. The motion of electron is described by the quantum mechanics equation given by

$$i\hbar\frac{\partial\Psi}{\partial t} = \left(-\frac{\hbar^2}{2m_e}\Delta + U\right)\Psi, \tag{6}$$

where Ψ is an electron wave function, and U is the potential created by the proton and sulfur ion S^{3+}. The system of classical equations (4) can be reduced to Newton's equations of motion for ions:

$$\begin{array}{l} m_1\frac{d\vec{v_1}}{dt} = \vec{F}_{12} + < \vec{F}_{1e} > \\ m_2\frac{d\vec{v_2}}{dt} = \vec{F}_{21} + < \vec{F}_{2e} > \end{array}, \tag{7}$$

where $\vec{F}_{12} = Z_1\, Z_2\, e^2\frac{\vec{R}_1-\vec{R}_2}{4\epsilon_0|\vec{R}_2-\vec{R}_1|^3}$, $\vec{F}_{21} = Z_1\, Z_2\, e^2\frac{\vec{R}_2-\vec{R}_1}{4\epsilon_0|\vec{R}_2-\vec{R}_1|^3}$ are the Coulombic forces of an interaction of ions with each other, and

$$\begin{array}{l} < \vec{F}_{1e} >= \frac{Z_1\, e^2}{4\epsilon_0} < \Psi|\frac{\vec{R}_1-\vec{r}}{|\vec{R}_1-\vec{r}|^3}\Psi > , \\ < \vec{F}_{2e} >= \frac{Z_2\, e^2}{4\epsilon_0} < \Psi|\frac{\vec{R}_2-\vec{r}}{|\vec{R}_2-\vec{r}|^3}\Psi > \end{array} \tag{8}$$

are the Coulombic forces of ion interactions with the electron cloud.

3. Fastest descent method for solving the stationary Schrödinger equation

In order to interpret the change of the electronic wave function with time in terms of eigenstates, it is required to know the eigenfunctions. Let us consider the stationary Schrödinger equation:

$$\hat{H}\Phi = E\Phi, \tag{9}$$

where $\Phi = \Phi\left(\overrightarrow{r}\right)$. The standard way to solve the stationary Schrödinger equation (9) is that its resolution can be found as a series over a complete set of known analytic functions $\Phi(\overrightarrow{r}) = \sum_{k=1}^{\infty} C_k\phi_k(\overrightarrow{r})$. These series are substituted in (9), then the equation (9) is reduced to a matrix form, and in consequence, the process of solving the Schrödinger equation is reduced to the problem of diagonalising the matrix operator, for which many quantum chemistry programs have already been written.

However, in our work, we solve the equation (6) by the FDMs suggested recently in [36], which may be more convenient for the solution of the considered collisional problem. Thus, we propose a simple and very effective numerical procedure that, when using FDMs, has certain advantages over the standard methods of solving equation (14). The potentials are calculated on the fly and do not have to be precalculated as it is in the case of using *ab initio* methods.

To explain this approach more easily, we use a geometric interpretation of the equation (9). Let us consider the function $\Phi\left(\overrightarrow{r}\right)$ as a vector of infinite-dimensional Hilbert space. Obviously, the $\hat{H}\Phi\left(\overrightarrow{r}\right)$ function is also a vector of the infinite-dimensional Hilbert space. If $\Phi\left(\overrightarrow{r}\right)$ is a solution to equation (9), then $\hat{H}\Phi\left(\overrightarrow{r}\right)$ is proportional to $\Phi\left(\overrightarrow{r}\right)$ with the coefficient E. In geometric terms, we can interpret this as parallelism of the vectors $\Phi\left(\overrightarrow{r}\right)$ and $\hat{H}\Phi\left(\overrightarrow{r}\right)$ in the infinite-dimensional Hilbert space.

Now, we consider some arbitrary vector $\Phi\left(\overrightarrow{r}\right)$ of the infinite-dimensional Hilbert space, which does not overall satisfy (9) and is not its solution. We calculate $\hat{H}\Phi\left(\overrightarrow{r}\right)$. The vector $\Phi\left(\overrightarrow{r}\right)$ of the infinite-dimensional Hilbert space can be represented as a sum $\Phi\left(\overrightarrow{r}\right) = \Phi_{\parallel}\left(\overrightarrow{r}\right) + \Phi_{\perp}\left(\overrightarrow{r}\right)$, where the vector $\Phi_{\parallel}\left(\overrightarrow{r}\right)$ is parallel to the vector $\hat{H}\Phi\left(\overrightarrow{r}\right)$, (that is, $\Phi_{\parallel}\left(\overrightarrow{r}\right)$ is proportional to $\hat{H}\Phi\left(\overrightarrow{r}\right)$) while $\Phi_{\perp}\left(\overrightarrow{r}\right)$ is an orthogonal complement to $\Phi_{\parallel}\left(\overrightarrow{r}\right)$ up to $\Phi\left(\overrightarrow{r}\right)$. Clearly, $\Phi_{\parallel}\left(\overrightarrow{r}\right) = \left\langle \frac{\hat{H}\Phi\left(\overrightarrow{r}\right)}{\left\|\hat{H}\Phi\left(\overrightarrow{r}\right)\right\|} \mid \Phi\left(\overrightarrow{r}\right) \right\rangle \frac{\hat{H}\Phi\left(\overrightarrow{r}\right)}{\left\|\hat{H}\Phi\left(\overrightarrow{r}\right)\right\|}$. With the help of subsequent transformations of the $\Phi\left(\overrightarrow{r}\right)$ function, one can obtain a function that will satisfy (9). Defining s as a parameter, let us consider the parametric transformation:

$$\Phi\left(\overrightarrow{r}, s+\triangle s\right) = \Phi\left(\overrightarrow{r}, s\right) - \alpha\left(s\right)\Bigg(\Phi\left(\overrightarrow{r}, s\right) + \\ - \left\langle \frac{\hat{H}\Phi\left(\overrightarrow{r}, s\right)}{\left\|\hat{H}\Phi\left(\overrightarrow{r}, s\right)\right\|} \mid \Phi\left(\overrightarrow{r}, s\right) \right\rangle \frac{\hat{H}\Phi\left(\overrightarrow{r}, s\right)}{\left\|\hat{H}\Phi\left(\overrightarrow{r}, s\right)\right\|} \Bigg) \triangle s, \tag{10}$$

where $\alpha\left(s\right) > 0$, and $\triangle s$ is assumed to be sufficiently small. The essence of transformation (10) is that component $\Phi_{\perp}\left(\overrightarrow{r}, s\right)$ is reduced in such a way that step by step we get closer to the solution to equation (9). Passing to the limit $\triangle s \to 0$, we can write transformation (10) in the form of a differential equation which solution approaches a solution to equation (9) with the increase of parameter s:

$$\frac{\partial\Phi\left(\overrightarrow{r}, s\right)}{\partial s} = \frac{\alpha\left(s\right)}{\left\|\hat{H}\Phi\left(\overrightarrow{r}, s\right)\right\|^2} \Big(\left\langle \hat{H}\Phi\left(\overrightarrow{r}, s\right) \mid \Phi\left(\overrightarrow{r}, s\right) \right\rangle \times \\ \hat{H}\Phi\left(\overrightarrow{r}, s\right) \Big) - \alpha\left(s\right)\Phi\left(\overrightarrow{r}, s\right). \tag{11}$$

To simplify equation (11), we use the fact that $\hat{H}\Phi\left(\overrightarrow{r}, s\right) \approx E(s)\Phi\left(\overrightarrow{r}, s\right)$, where $E(s) = \left\langle \hat{H}\Phi\left(\overrightarrow{r}, s\right) \mid \Phi\left(\overrightarrow{r}, s\right) \right\rangle$. We also take into account that the discrete spectrum state energies are negative, thus we can conveniently take $\alpha\left(s\right) = -E(s) > 0$. Then equation (11) can be expressed in a particularly simple form [36]:

$$\frac{\partial\Phi\left(\overrightarrow{r}, s\right)}{\partial s} = -\left(\hat{H}\Phi\left(\overrightarrow{r}, s\right) - E\left(s\right)\Phi\left(\overrightarrow{r}, s\right) \right), \tag{12}$$

$$E(s) = \left\langle \hat{H}\Phi\left(\overrightarrow{r}, s\right) \mid \Phi\left(\overrightarrow{r}, s\right) \right\rangle. \tag{13}$$

The ground stationary state of the Schrödinger equation can be calculated through the limit $\Phi_0\left(\overrightarrow{r}\right) = \lim_{s\to\infty}\Phi\left(\overrightarrow{r}, s\right)$ of the solution to equation (12), and, accordingly, the ground state energy is calculated through the $E_0 = \lim_{s\to\infty} E\left(s\right)$ limit.

To calculate the excited states, one must supplement equation (12) (with the requirement of orthogonality) of the newly computed states to those already computed. The easiest way to perform such an implementation is to modify equation (12) in the following way: if all states up to the $(j-1)$ state have already been calculated, the

next state can be found through the limit when $s \to \infty$ of a solution the equation,

$$\frac{\partial \Phi_j\left(\overrightarrow{r}, s\right)}{ds} = -\left(\hat{H}\Phi_j\left(\overrightarrow{r}, s\right) - E_j\left(s\right)\Phi_j\left(\overrightarrow{r}, s\right)\right) + \\ + \sum_{i=0}^{j-1} \lambda_{ji}(s)\,\Phi_i\left(\overrightarrow{r}\right), \tag{14}$$

$$E_j(s) = \left\langle \hat{H}\Phi_j\left(\overrightarrow{r}, s\right) \mid \Phi_j\left(\overrightarrow{r}, s\right)\right\rangle, \tag{15}$$

$$\lambda_{ji}(s) = \left\langle \Phi_i\left(\overrightarrow{r}\right) \mid \hat{H}\Phi_j(\overrightarrow{r}, s)\right\rangle. \tag{16}$$

It is worth bearing in mind that equations (12) and (14), with some fine distinctions, can be classified into the category of equations for expressing heat conduction. For this type of equation, very fast finite-difference techniques have already been developed, so they can be used effectively in numerical codes. Therefore, equations (12) and (14) can be written in a very convenient and simple form to calculate the ground and excited states of the system. The details of the mathematical development of the methods are described below.

The virtue of equations (12) and (14) for calculating the ground and the excited states consists in the universality and simplicity of the approach (the calculations can be performed equally for almost any potential) and in the fast calculation algorithm. However, the disadvantage of the approach is that when calculating the eigenfunctions as a series over some full set of functions and reducing the problem to the matrix one, it is possible to improve accuracy through a very successful choice of basis functions, while with the finite difference approach, the accuracy can be increased only through a fine grid. However, achieving acceptable accuracy with equations (12) and (14) is relatively simple, and the method is very versatile.

Both equations (12) and (14) can also be derived directly from the variational principle. For this purpose, using the Lagrange method, we compose a functional:

$$\Pi = \sum_{\Omega} \Phi_{klm}\left[\left(-\frac{\hbar^2}{2m_e}\Delta_{klm} + U_{klm}\right)\Phi_{klm}\right]a^3 + \\ -\mu\left(\sum_{\Omega}\Phi_{klm}^2 a^3 - 1\right), \tag{17}$$

which is a finite-difference approximation of the functional $\left\langle \Phi \mid \hat{H}\Phi\right\rangle - \mu\left(\langle\Phi \mid \Phi\rangle - 1\right)$ to be minimized. Here, μ is a Lagrange multiplier and Δ_{klm} is a finite-difference approximation of operator Δ. The fastest descent equations $\frac{\partial}{\partial s}\Phi_{klm}a^3 = -\frac{\partial \Pi}{\partial \Phi_{klm}}$ lead to a difference analogue of equation (12). The Lagrange multiplier μ is determined from the condition $\frac{\partial}{\partial s}\sum_{\Omega}\Phi_{klm}^2 a^3 = -\sum \Phi_{klm}\frac{\partial \Pi}{\partial \Phi_{klm}} = 0$, which leads to $\mu = \sum_{\Omega}\Phi_{klm}\left[\left(-\frac{\hbar^2}{2m_e}\Delta_{klm} + U_{klm}\right)\Phi_{klm}\right]a^3$, which is a discrete approximation of the energy E. The difference analog of equation (14) is derived similarly, with the additional condition of orthogonality of the excited states to each other. Since equations (12) and (14) can be obtained from the FDM, we can call them "the fastest descent equations".

4. Computational method

The system of equations (6) and (7), which describes the dynamics of the considered system of three particles, is solved numerically by using FDM. In the context of ion-atom collisions, it provides a computational approach to simulate the complex dynamics of charge transfer between the colliding species. It allows us to model these interactions by discretizing the spatial and temporal dimensions, breaking down the system into a grid, and calculating the changes in charge distribution over time t. The region of interest, where the collision occurs, is discretized into a grid. Each grid point represents a specific spatial location. Therefore, in the three-dimensional space, we introduce the grid $\Omega = \{(x_k, y_l, z_m)\}$, where $x_{k+1} = x_k + a$; $y_{l+1} = y_l + a$; $z_{m+1} = z_m + a$; $k, l, m = 0, 1, 2, \cdots, N$ and where a is a grid step. Next, we approximate equation (6) with a system of differential equations

$$i\hbar \frac{\partial \Psi_{klm}}{\partial t} = \left(-\frac{\hbar^2}{2m_e} \Delta_{klm} + U_{klm} \right) \Psi_{klm}, \tag{18}$$

where $\Psi_{klm}(t) = \Psi(x_{k,} y_l, z_m, t)$,

$$U_{klm} = \frac{\int_{\omega_{klm}} U(x', y', x')\, dx' dy' dz'}{\int_{\omega_{klm}} dx' dy' dz'}, \tag{19}$$

and

$$\begin{aligned} \triangle_{klm} \Psi_{klm} = & \frac{\Psi_{k+1,lm} - 2\Psi_{klm} + \Psi_{k-1,lm}}{a^2} + \\ & \frac{\Psi_{k,l+1,m} - 2\Psi_{klm} + \Psi_{k,l-1,m}}{a^2} + \\ & \frac{\Psi_{kl,m+1} - 2\Psi_{klm} + \Psi_{kl,m-1}}{a^2}. \end{aligned} \tag{20}$$

In (19), ω_{klm} is a cube with the edge a: $\omega_{klm} = \{(x, y, z) : x_k - \frac{a}{2} < x < x_k + \frac{a}{2}, y_l - \frac{a}{2} < y < y_l + \frac{a}{2}, z_m - \frac{a}{2} < z < z_m + \frac{a}{2}\}$. Thus, in (19), we have regularised potential U. Regularising potential U in the numerical calculations is necessary since the given potential U has singularities at the points of the position of the ions, and, therefore, an integral of this potential U over a domain does not exist in the usual sense. However, this integral exists as an improper integral, in the so-called the Lyapunov sense [37] [38], and can be calculated by potential regularization. Next, we supply equations (18) with natural boundary conditions $\lfloor \Psi_{klm} \rfloor_{\partial\Omega} = 0$, where $\partial\Omega$ is the boundary of domain Ω. Moreover, the system of ordinary differential equations (18) and (7) is self-consistently solved by the well-known second-order Runge–Kutta method, and the solution describes the process of particles colliding.

The numerical scheme we use conserves the norm. The global error of the method is proportional to $O(\tau^2 + a^2)$. The condition for the time step τ and space step a, $\tau \ll \frac{m_e}{\hbar} a^2$, ensures the stability of the solution of the Schrodinger equation. The numerical parameters employed in the simulations are collected in Table 1.

Table 1. Numerical parameters used in the calculations.

Variable	Value	Description
N_x	100	Number of grid points OX direction
N_y	100	Number of grid points OY direction
N_z	100	Number of grid points OZ direction
a	0.25 a.u.	Spacing step
b	$[0, 7.5]$ a.u.	Range of impact parameters
τ	10^{-4} fs	Time increment of the propagation

5. Collisional dynamics

5.1. Initial condition.

The initial conditions are given by the masses m_J, positions $\overrightarrow{R}_J$ and initial velocities $\overrightarrow{v}_J$ of hydrogen H^+ and sulfur S^{3+} ions. In the article, the position and velocity components of the hydrogen are indicated with the index H ($\overrightarrow{r}_H$, $\overrightarrow{v}_H$), while the position and velocity components of the sulfur ion as ($\overrightarrow{r}_S$, $\overrightarrow{v}_S$). We consider the following initial conditions $\overrightarrow{r}_H = (r_{Hx}, r_{Hy}, r_{Hz}) = (-7.5, 0, b_z)$ a.u., $\overrightarrow{v}_H = (v_{Hx}, v_{Hy}, v_{Hz}) = (v_x, 0, 0)$ m/s, $\overrightarrow{r}_S = (r_{Sx}, r_{Sy}, r_{Sz}) = (2.5, 0, 0)$ a.u., $\overrightarrow{v}_S = (v_{Sx}, v_{Sy}, v_{Sz}) = (0, 0, 0)$ m/s. In the following, the results for different values of b_z and v_x will be analyzed. The calculations were carried out with a difference grid step a and equal to 1/4 of the bohr radius, and with a time step $\tau = 0.05 \cdot \frac{m_e}{\hbar} \cdot a^2 \sim 10^{-19}$s. Time step τ is determined from considerations of stability and convergence of the numerical method. Below, head-on ion-atom collision and an influence of impact parameter will be discussed.

5.2. Head-on ion-atom collision

This is a type of collision between an ion and an atom where the interaction occurs primarily in the central region of the collision, meaning that the impact parameter $\overrightarrow{b}$ is close to zero. The impact parameter $\overrightarrow{b}$ is the perpendicular distance between the initial positions of the center of mass of the ion and the target atom at the moment when they are infinitely separated. Initially, both $S^{3+}(3s^2 3p)$ and $H(1s)$ have their own sets of eigenstates, corresponding to their individual electron configurations and energy levels. The initial condition $\Psi_{klm}(t = 0)$ is set using a well-known analytical solution for the ground state of the H (1s) atom. The conditions $\overrightarrow{r}_H(t = 0)$, $\overrightarrow{r}_S(t = 0)$, $\overrightarrow{v}_H(t = 0)$, and $\overrightarrow{v}_S(t = 0)$ for ions are set in such a way that the particles collide after given time. In order to present the different spatial behaviour of the interaction in the head-on collision, we specified several situations. The initial distance between the ions is chosen for $R = 10$ a.u. for all the considered cases.

Firstly, we investigated the situation where the initial velocity v at which the H approaches the S^{3+} is $v_H = 50\ 000$ m/s, which corresponds to a kinetic energy of about $E = 13$ eV. The results of the numerical simulation of the evolution of the electron cloud in the system for selected times t are presented as snapshots in Fig.1. The electron density motion should be observed by following the individual rows in the figure. At the beginning, the electron cloud is located near the H ion. As S^{3+} and H approach each other during the collision, the landscape of interaction changes, and the probability of finding a common electron cloud increases. When the ions are located at a distance of approximately $R = 5$ a.u. a part of the electron cloud moves to the vicinity of the S^{3+}. Within the increase of the evolution time, the interaction between

the electrons of the system leads to the formation of a combined electron cloud, and the electron states become entangled. The smallest distance at which ions approach is $R_{min} = 2.5$ a.u. (the collision occurs at a time of around $t = 9$ fs). In the final stage of the process, which takes place within several fs, the hydrogen ion and the electron move away from the sulfur ion. As a result, the electron returns to the ground state of the H(1s) atom. That is, the ground state of the H(1s) is restored. Actually, we only note that the ions in the collision process do not approach very closely due to the manifestation of the Coulomb law and the repulsion of ions when they approach.

The head-on collision was investigated also for the higher velocity of the v_H =250 000

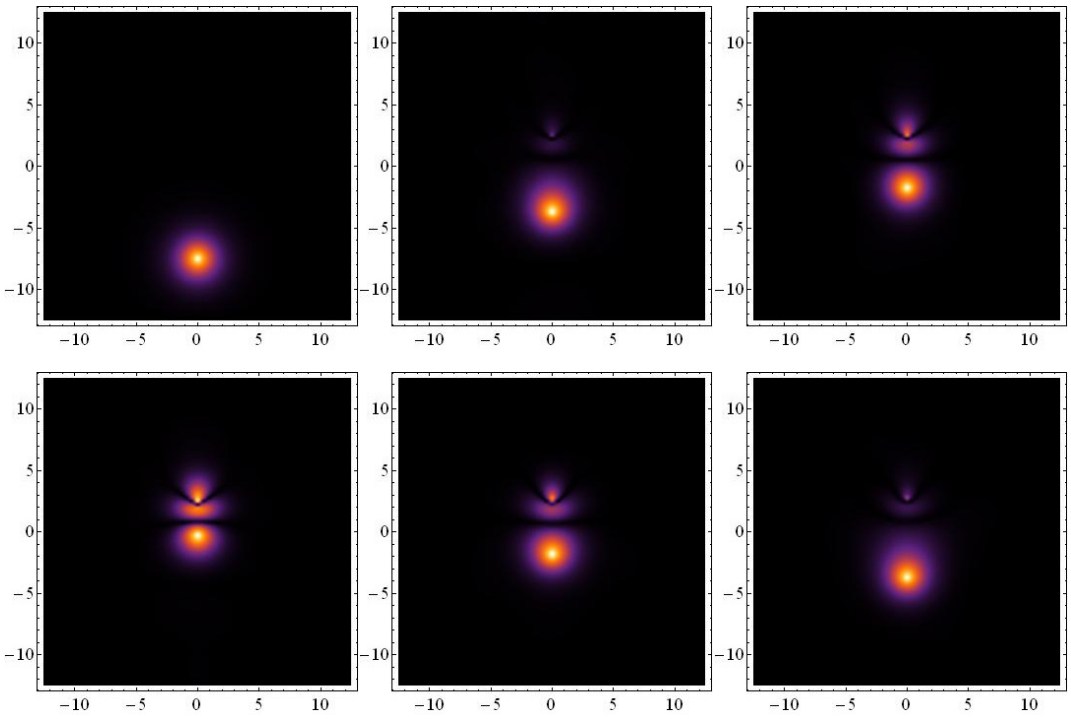

Figure 1. Evolution of the electron cloud $|\Psi|$ during the head-on collision for $E = 13$ eV and given times (starting from top left in the first row): $t = 0$ fs, $t = 4$ fs, $t = 6$ fs, $t = 8$ fs, $t = 12$ fs and $t = 14$ fs. The scale of the axes in the graphics is given in a.u.

m/s, corresponding to $E = 325$ eV. At this energy scale, various processes can occur in ion-atom collision. Moreover, at 325 eV, the collision energy may be sufficient to ionize the hydrogen atom as well as lead to the removal of one or more electrons. It can result in the creation of positively charged H^+ and free electrons, each carrying energy proportional to the collision energy. The chosen snapshots of the simulation are given in Fig.2.

Indeed, following the process of the evolution of electron cloud as the distance between the ions decreases, an interesting pattern can be observed. The electron cloud of hydrogen ion moves towards S^{3+} and, eventually, in a sufficient distance R and time t, creates the joint electron cloud. The closest distance R_{min} between the particles is estimated for 0.3 a.u. and reached at time $t = 2$ fs. The electron cloud is spread in the region of interaction showing that the collision energy can also be transferred to the electrons of H, causing them to move to higher energy states (ionization). It can be also noticed that after the collision within just a few femtoseconds, part of electron cloud remains at S^{2+} ion.

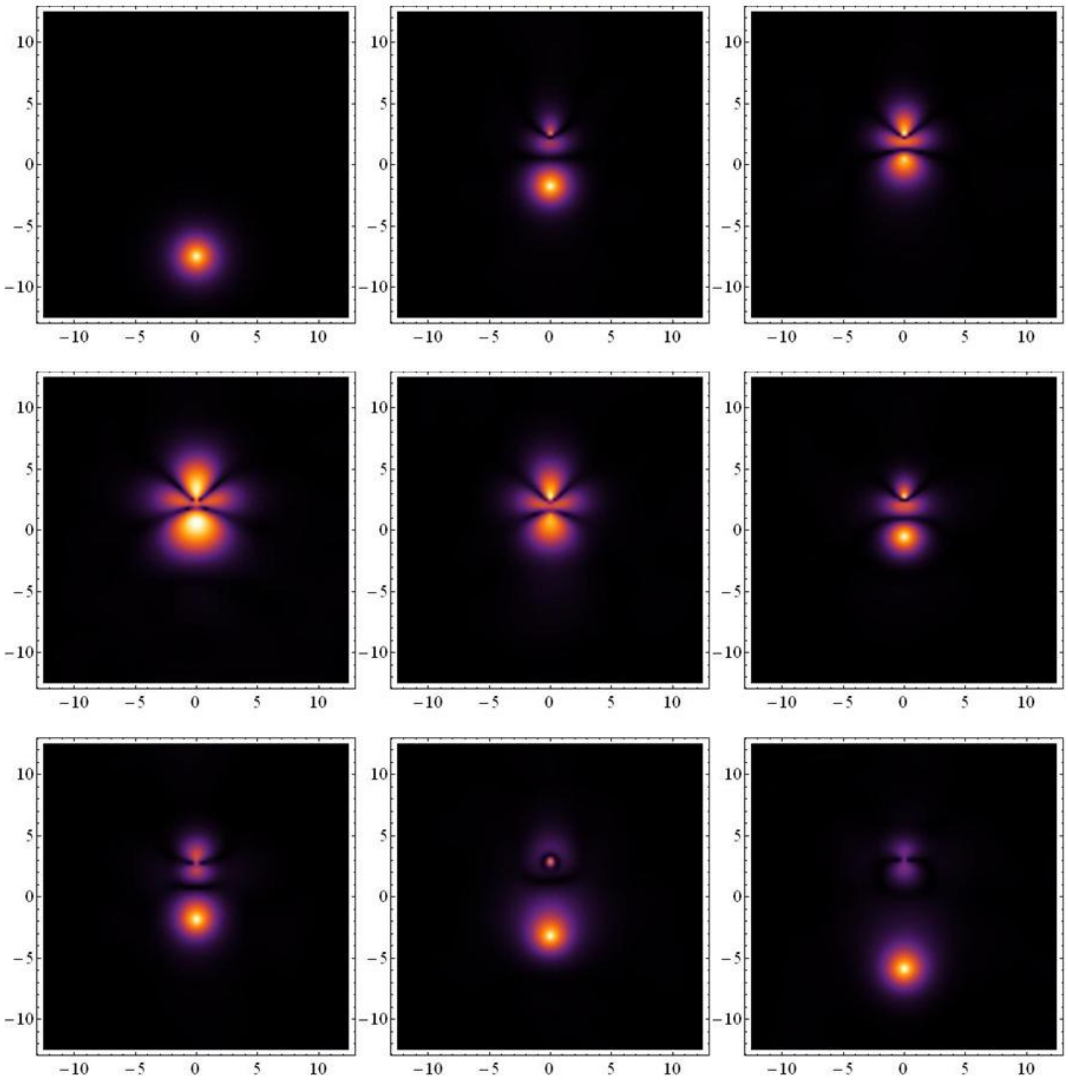

Figure 2. Evolution of the electron cloud $|\Psi|$ during the head-on collision for $E = 325$ eV and given times (starting from top left in the first row): $t = 0$ fs, $t = 1$ fs, $t = 1.7$ fs, $t = 2$ fs, $t = 2.5$ fs, $t = 2.9$ fs, $t = 3.2$ fs, $t = 3.5$ fs and $t = 4$ fs. The scale of the axes in the graphics is given in a.u.

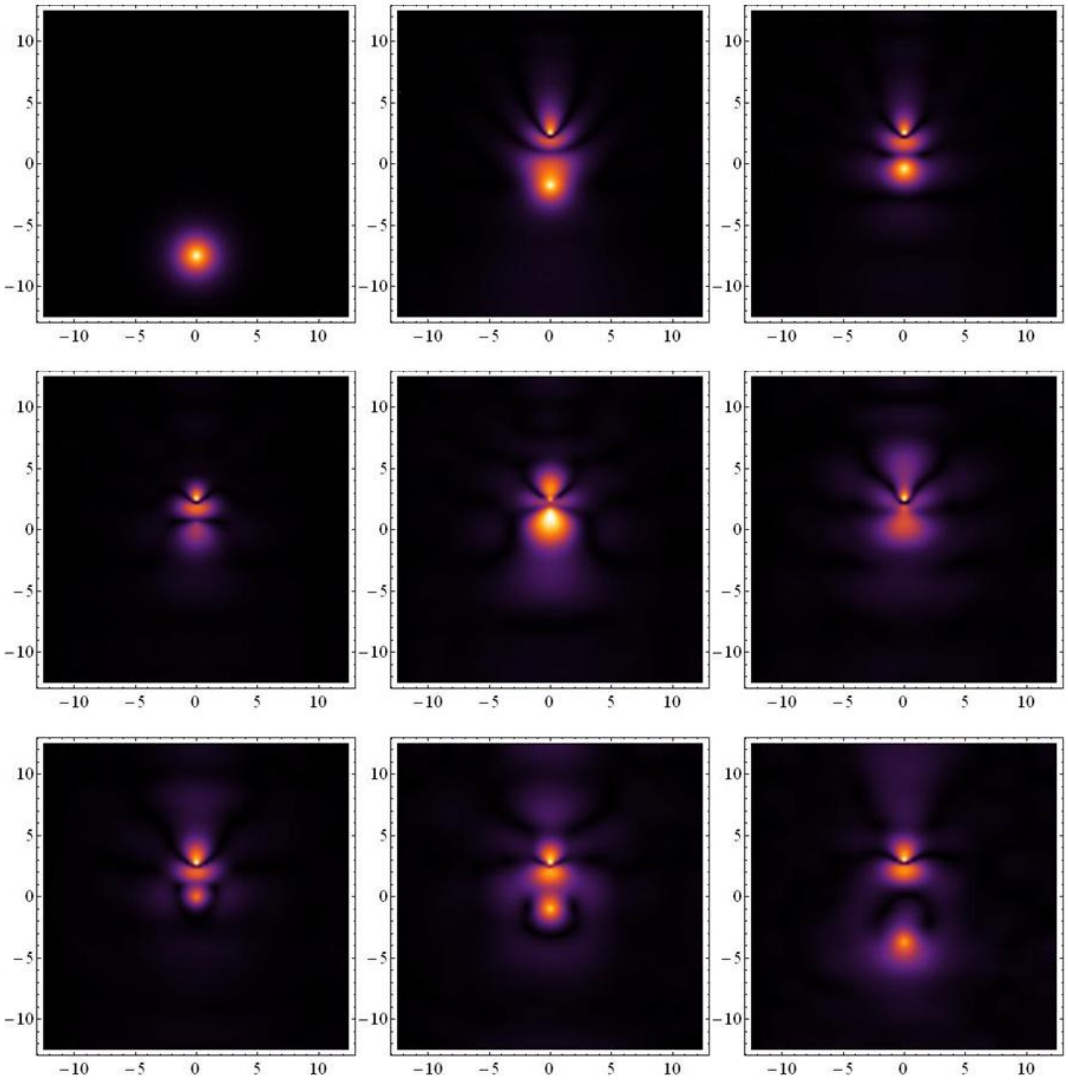

Figure 3. Evolution of the electron cloud $|\Psi|$ during the head-on collision for $E = 5$ keV and given times (starting from top left in the first row): $t = 0$ fs, $t = 3 \cdot 10^{-1}$ fs, $t = 3.8 \cdot 10^{-1}$ fs, $t = 4.3 \cdot 10^{-1}$ fs, $t = 4.8 \cdot 10^{-1}$ fs, $t = 5.8 \cdot 10^{-1}$ fs, $t = 6.8 \cdot 10^{-1}$ fs, $t = 7.3 \cdot 10^{-1}$ fs, $t = 8.8 \cdot 10^{-1}$ fs. The scale of the axes in the graphics is given in a.u.

Additionally, the trajectory of the high-energy ion was characterized by increased velocity and penetration depth into the atomic structure. At keVs, the possibility of multiple scattering events increases. Indeed, the increased velocity up to $v_H = 1 \cdot 10^6$ m/s results in the situation, that the hydrogen ion possesses a significantly higher kinetic energy (corresponding to the value of $E = 5$ keV) and causes more pronounced charge transfer, ionization, and excitation processes. This can lead to more complex angular distributions, especially at larger scattering angles. The ion's electron cloud trajectory can result in a more penetrative and dynamic interaction as can be observed in the snapshots of Fig.3 with the evolution of the electron density. Indeed, the process takes place at a very short time scale (much below 1 fs). The scattering pattern exhibits a relatively rich distribution of electron cloud which is strongly influenced by the Coulombic interaction between the charged particles at keV energy range. At the final stage of the simulation we can observe a substantial part of the electron cloud remains on sulfur ion. The detailed inspection of the results indicates that, as expected, we can observe a transfer of electron leading to the $S^{2+} - H^+$ configuration of the system. Moreover, in such a situation, the electrons may be promoted to higher energy levels, resulting in the release of photons.

5.3. Influence of impact parameter

In ion-atom collisions, the impact parameter is a key parameter that describes the spatial orientation and distance between the ion and the target atom as they approach each other. The impact parameter plays a crucial role in determining the outcome of the collision, influencing the trajectory and the probability of various collision processes. In order to determine the effect of the change of the impact parameter for different ranges of collision energy (from eV to keV) we investigated several possibilities. Firstly, a situation of the collision for the $E = 13$ eV and $b = 2.5$ a.u. was consequently analyzed. Based on the results of the calculations, a schematic illustration of the collision for the considered situation is presented in Fig.4. It shows the evolution of the motion of H^+ over time.

Analysing the details of the collision process in Fig.5, it can be seen that the electron cloud behavior on the hydrogen ion changes compared to the head-on collision. At the beginning, electron cloud of H is moving along OX axis. When ions are approaching each other, both parts of the electron cloud start to interact and the potential energy landscape between the ion and the atom evolves. Indeed, the electrostatic interaction dominates at short distances, influencing the scattering patterns and outcomes. The electron cloud interacts with the sulfur ion and its surroundings during the collision (the probability of finding an electron cloud near the sulfur ion is non-zero), but after the collision the electron cloud moves away from the sulfur ion together with the hydrogen ion. The closest distance between ions is evaluated for $R_{min} = 3$ a.u. and collision takes place for a time around $t = 10$ fs. In order to evaluate the nature of the interaction, the scattering angle θ was calculated, which is estimated for $\theta = 1.0$ radian for this case. The dependence of impact parameters between $b \in [0, 7.5]$ a.u. on the values of R_{min} and θ angles for a collision energy of $E = 13$ eV obtained from performed calculations is given in the Table 2. As expected, with an increase of values of impact parameters we can observe a decrease in the scattering angles θ as presented in Fig.6.

Effect of the impact parameter was also investigated for a higher range of energy, such as $E = 325$ eV. The illustration of the evolution of electron cloud for $b = 2.5$

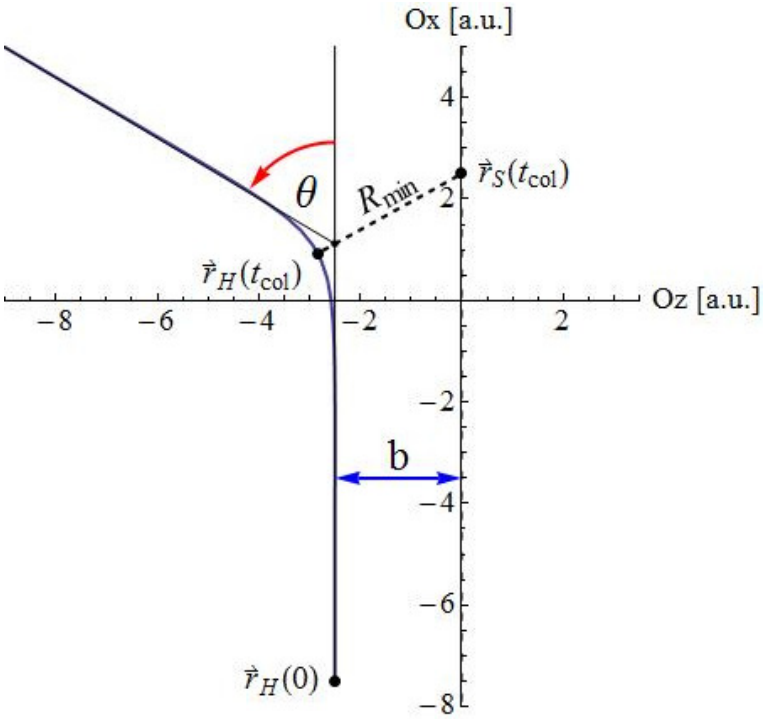

Figure 4. Illustration showing the trajectory of a H ion during the collision with a S^{3+} ion for impact parameter $b = 2.5$ a.u. and collision energy of $E = 13$ eV. t_{col} is the time at which the ions are the closest (where $\vec{r}_H(0)$ means the initial position of the H ion, and $\vec{r}_H(t_{col})$ and $\vec{r}_S(t_{col})$ - the positions of both ions, respectively at R_{min} -the minimum distance between them). Using these relationships, the scattering angle θ was determined.

Table 2. Dependence of the minimum distance between ions (R_{min}) and scattering angle (θ) on impact parameters for collision energy 13eV.

b [a.u.]	0.0	0.5	1.0	1.5	2.0	2.5	3.0	3.5	4.0	5.0	6.0	7.5
R_{min} [a.u.]	2.6	2.6	2.7	2.8	3.0	3.3	3.5	3.8	4.2	5.0	6.0	7.5
θ [radians]	3.1	2.7	2.2	1.7	1.3	1.0	0.7	0.5	0.3	0.0	0.0	0.0

a.u. is displayed in Fig.7. Indeed, as it was in the case of the head-on collision, the electron cloud of hydrogen ion with the increase of the distance R shows less abundant scattering pattern. Since no internal energy changes within the simulation time, the transition probability increases as energy is raised. The interaction between particles takes place at $t = 2$ fs and the closest distance is $R_{min} = 2.5$ a.u. After the collision, part of the electron cloud remains on sulfur, however with much less probability. Moreover, by sequential increasing the impact parameter up to $b = 5$ a.u., the electron cloud experiences even less interaction, leading to almost entirely elastic scattering. Moreover, the potential energy landscape between the ion and the atom evolves dynamically, with the electrostatic interaction dominating at short distances.

On the other hand, at higher (keV range) energies, the impact parameter continues to play a crucial role and influences the probability of various scattering events. At $E = 5$ keV charge transfer processes become increasingly significant, and ionization is likely to occur more frequently. Electrons may be transferred between the ion and the atom, and the ionization of inner-shell electrons becomes more pronounced. Therefore, at keVs, the collision dynamics are more complex, and multiple interactions can occur. By following the results of performed calculations for the different impact parameters

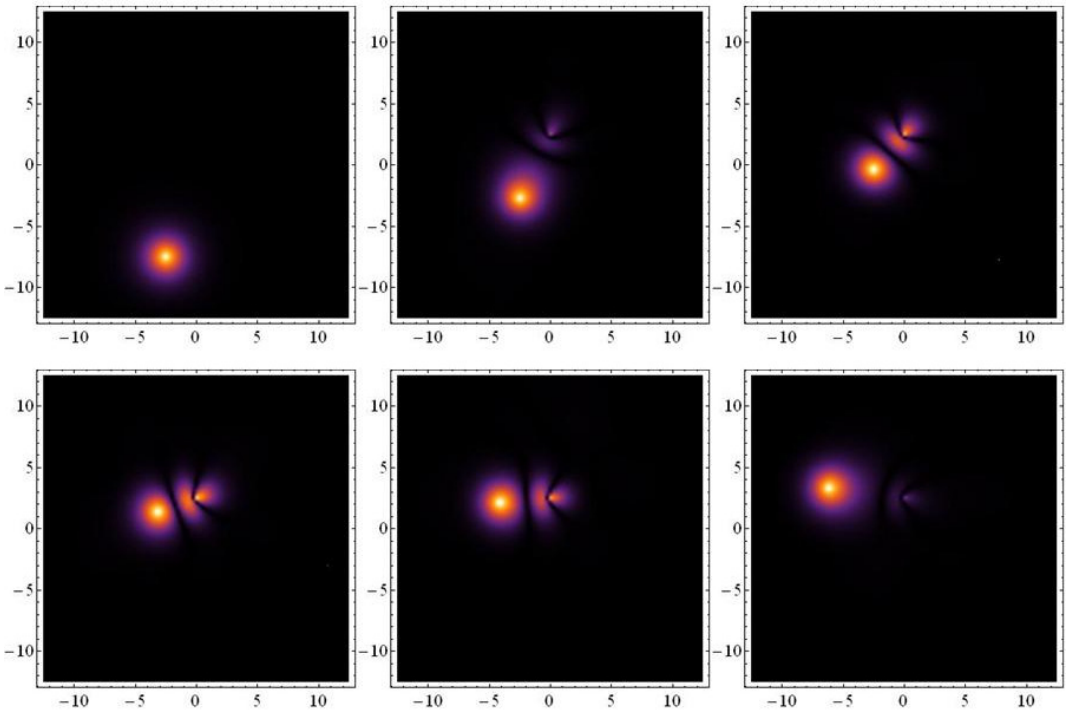

Figure 5. Evolution of the electron cloud $|\Psi|$ during the collision with impact parameter $b = 2.5$ a.u. for energy $E = 13$ eV and given times (starting from top left in the first row): $t = 0$ fs, $t = 5$ fs, $t = 7.5$ fs, $t = 10$ fs, $t = 11.5$ fs and $t = 14$ fs. The scale of the axes in the graphics is given in a.u.

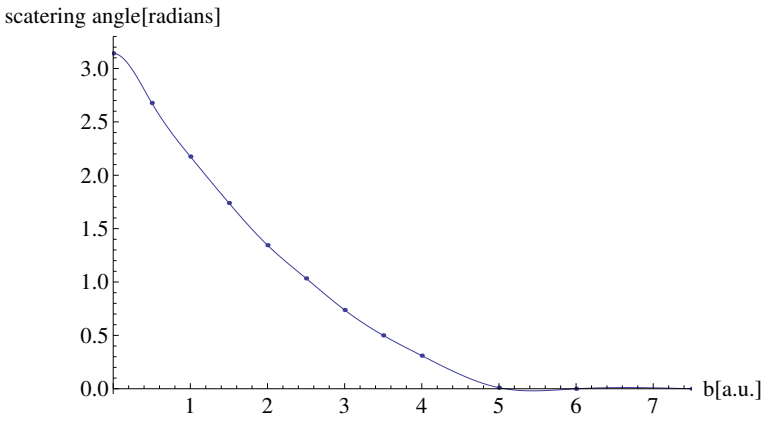

Figure 6. Dependence of scattering angle (in radians) on impact parameter.

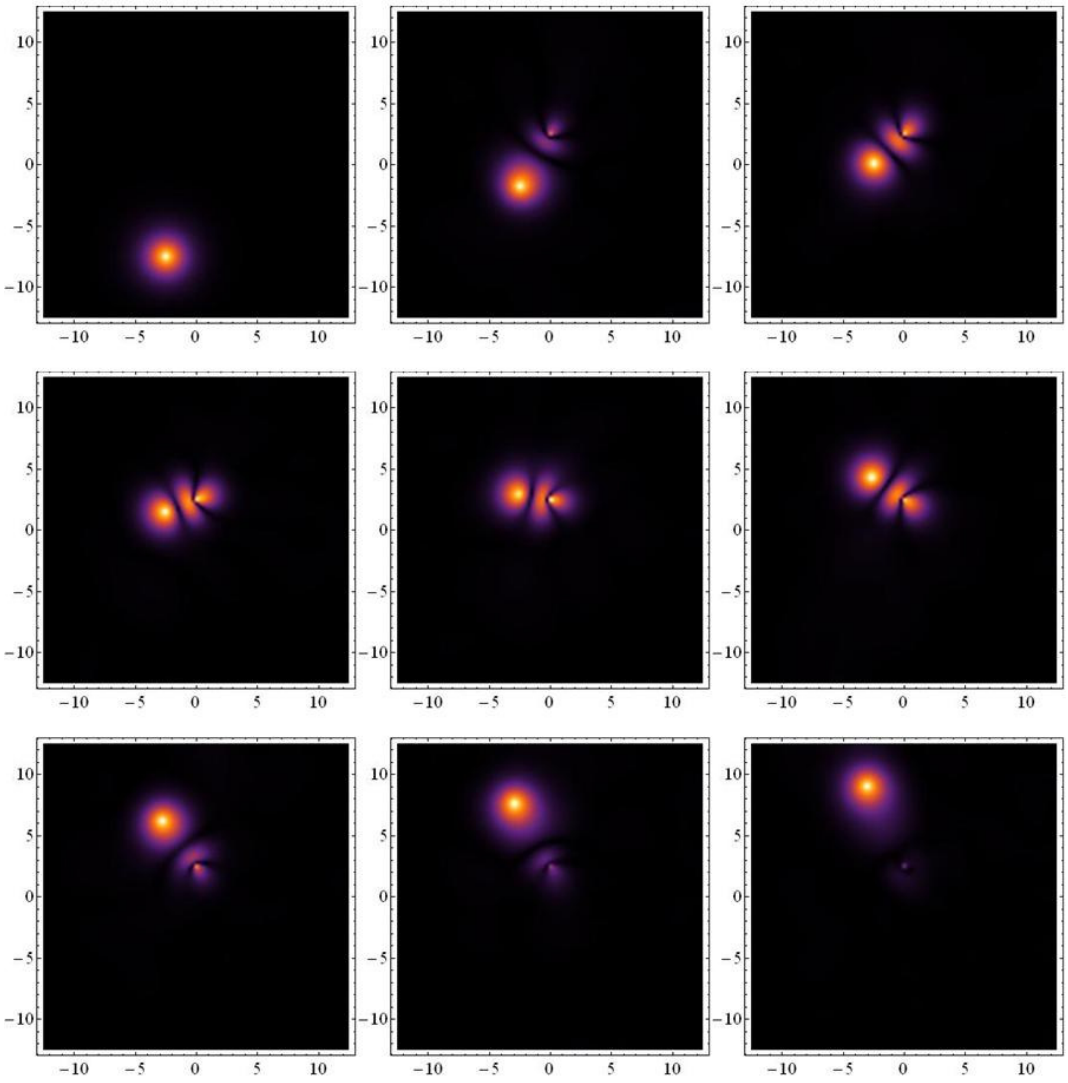

Figure 7. Evolution of the electron cloud $|\Psi|$ during the collision with impact parameter $b = 2.5$ a.u. for energy $E = 325$ eV and given times (starting from top left in the first row): $t = 0$ fs, $t = 1$ fs, $t = 1.9$ fs, $t = 2.2$ fs, $t = 2.5$ fs, $t = 2.9$ fs, $t = 3.2$ fs and $t = 3.5$ fs. The scale of the axes in the graphics is given in a.u.

of $b \in [0, 5]$ a.u. we can observe that the choice of the impact parameter was large enough so that the amount of the electron cloud on the exit of the interaction no longer changes. Indeed, the transition probability increases with the energy since the interaction region is completely covered. This is consistent with the fact that, for the given energy value of $E = 5$ keV a common process is elastic scattering, where the kinetic energy of the scattered particles remains unchanged. As a result, we observed the angular distribution in the forward direction, which is typically observed for elastic scattering.

In summary, by applying our model of the collision for different examples we show, that specific outcomes of the collisions depend not only on the energy range of the collision but also on the impact parameter. The impact parameter influences the scattering angle θ and determines the collision processes that may occur. Inelastic scattering affects the probability of the various inelastic processes and in the case of elastic scattering, where there is no change in internal states, influences the deflection angle of the ion. On the other hand, the likelihood of capture processes depends strongly on the impact parameter as well.

6. Interpretation of particle collisions in terms of eigenstates depending on the distance between ions.

For the $S^{3+} - H^{+}-$ electron system, where the sulfur ion is located at a distance of $R = 10$ a.u. from the hydrogen ion, the first five energy states of the electron are represented by the states $1s$, $2s$, $2p_x$, $2p_y$, $2p_z$ for the sulfur ion, respectively, while the sixth energy state of the electron corresponds to the ground state of H(1s) atom. The first energy state corresponds to the state with the lowest energy, and the subsequent states correspond to those with higher energies. The form of the first six eigenstates of the electron, for the position of the ions consistent with the initial condition ($\overrightarrow{r}_H = (-7.5, 0, 0)$ a.u., $\overrightarrow{r}_S = (2.5, 0, 0)$ a.u.) obtained based on the equations from the section 3, is presented in Fig. 8. When the distance between ions changes, these states change. The following section will consider the possibility of decomposing the solution of the time-dependent Schrödinger equation, representing the head-on collision of sulfur and hydrogen ions with an energy of $E = 13$ eV, into the first six energy states. Later in the section, general conclusions for other values of collision energies E will be provided.

6.1. Analysis of the model

Knowing the stationary states of the quantum system, depending on the distance R between the ions, we may understand the behaviour of the electron cloud during the collision process in terms of eigenstates. At the initial time instant, the electron cloud was concentrated around a hydrogen ion. It is illustrated in Fig.1 where at the initial time instant, the electron was in the 6th state of the hydrogen-sulfur system. It also means that the electron initially has fairly significant energy, corresponding to the electron energy in the hydrogen atom.

Let us calculate the expansion coefficients $\alpha_n(t) = \langle \Phi_n(\vec{R}(t)), \Psi(\vec{r}, t) \rangle$ of the dynamic wave function $\Psi(\vec{r}, t)$ in terms of the calculated calculated for the first six energy states $\Phi_n(\vec{R(t)})$ depending on the distance $R(t)$ between the ions. Then we

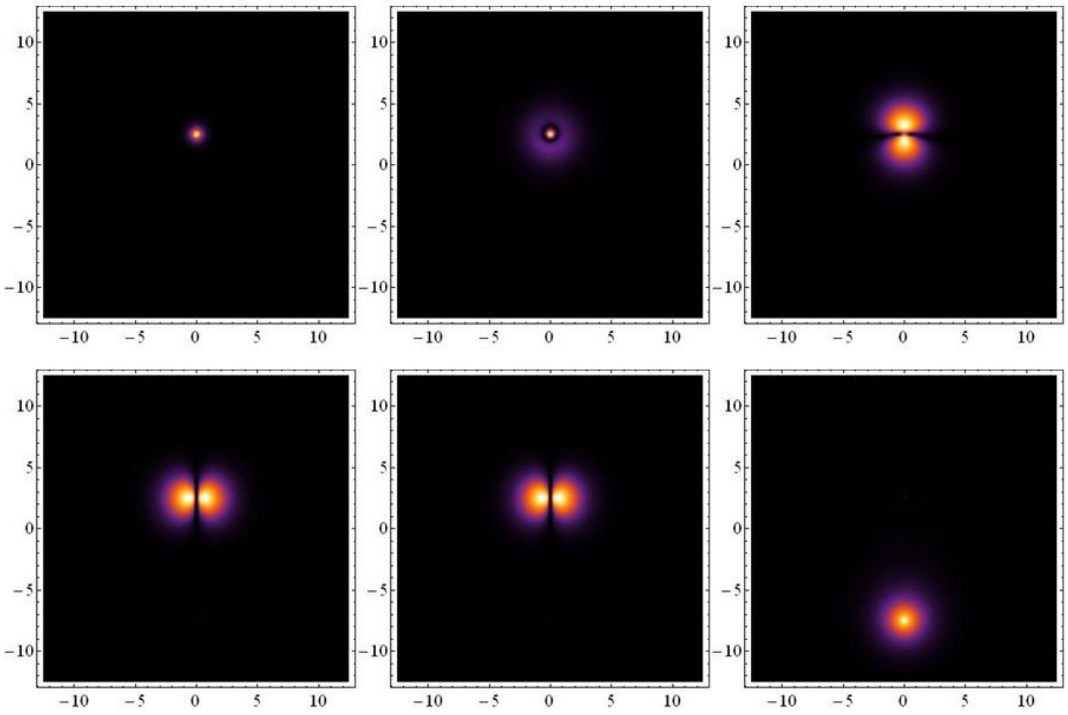

Figure 8. The absolute value of the Φ_n corresponding to the first six electron energy states, which are solutions of the stationary Schrodinger equation with the potential coming from the system $S^{3+} - H^{+}$ and ion positions $\overrightarrow{r}_H = (-7.5, 0, 0)$ a.u., $\overrightarrow{r}_S = (2.5, 0, 0)$ a.u. obtained on the $y = 0$ a.u. (energy levels E corresponding to energy states are equal $[-134.4, -35.7, -33.8, -33.8, -33.8, -21.8]$ eV). The scale of the axes in the graphics is given in a.u.

calculate the number

$$S(t) = \sum_{n=1}^{6} |\alpha_n(t)|^2, \tag{21}$$

which is an analog of the number Π characterising the completeness of a set of basis functions and is introduced in Parseval's theorem. For simplicity, we name Π the Parseval's number [39]. As one knows, for the system of basis functions to be complete, the relation $\Pi = 1$ is necessary. Calculations have shown that in our case, $0.99 \leq S(t) < 1$. That is, always, at any time instant, $S(t) \approx 1$. Therefore, the six calculated eigenfunctions to a very good approximation are always sufficient to interpret the behaviour of the wave function $\Psi(\vec{r}, t)$ during the collision in terms of the calculated eigenstates $\Phi_n(\vec{R}(t))$. The results for changes in the modulus of the expansion coefficients ($|\alpha_n(t)|$) of the first six energy states in time, obtained for head-on collision of ions with an energy of $E = 13$ eV are presented in Fig.9.

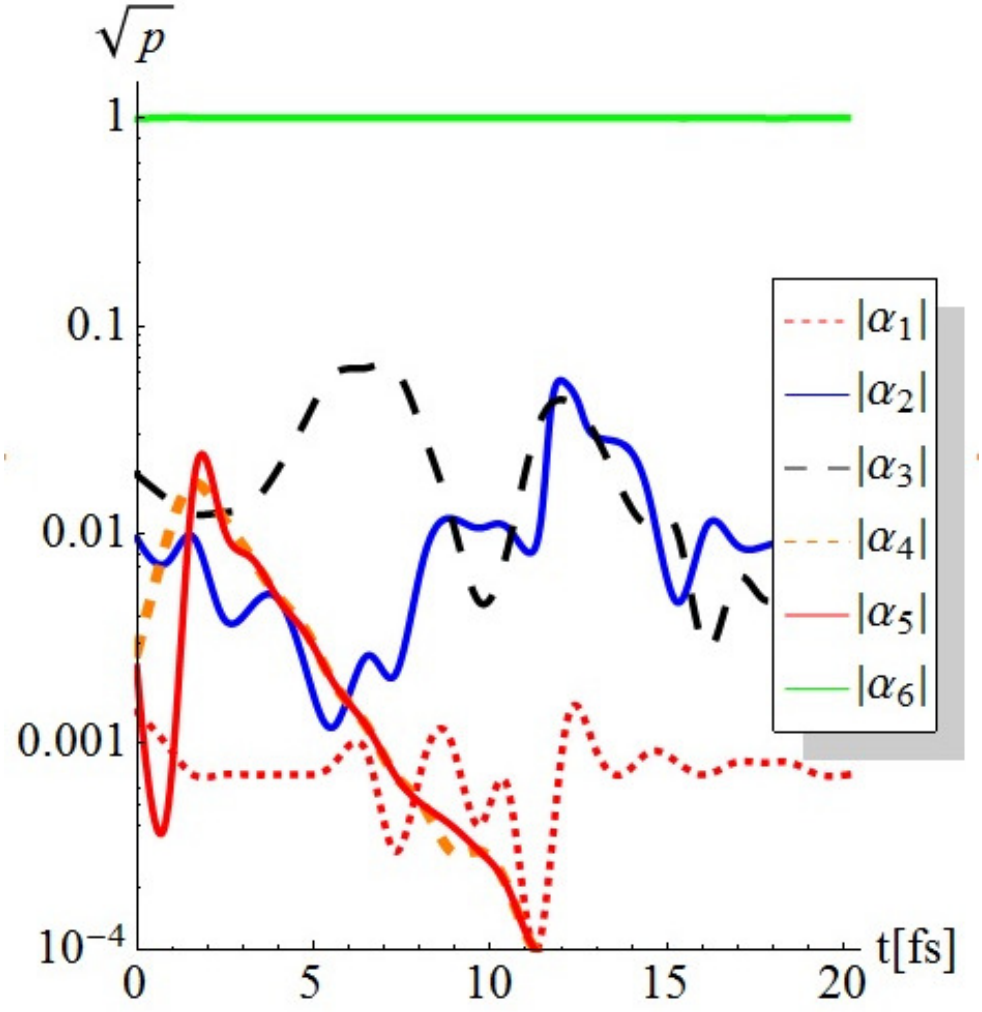

Figure 9. Time dependence of the absolute value of the α_n corresponding to the first six electron energy states.

The first five coefficients $\alpha_n(t)$ satisfy $|\alpha_n(t)| < 6 \cdot 10^{-2}$ for all t. Therefore, the first five calculated energy states $\Phi_n(\vec{R}(t))$ of the $S^{3+} - H^+$ system are practically uninvolved in the collision process. This is one of the very important arguments for the idea that the sulfur ion potential can be approximately considered as a Coulomb one, and this question will be analysed in more detail below. Of course, it might not be superfluous to take into account the deviation of the potential of the S^{3+} ion from the Coulomb one. However, using a pseudopotential for the S^{3+} ion may not give a significant refinement. The hydrogen ion approaches the sulfur ion, polarising the valence electron shell. Therefore, the correction to the Coulomb potential of the S^{3+} ion is probably dynamic, and understanding the dynamics of the process in the approximation used here may be useful for suggesting some corrections.

To discuss the applicability of the Coulomb approximation for the ion S^{3+} potential, further we consider the energies E_n of electrons of the $n-$th energy level of sulfur. We introduce also the effective radius $R_{S,n}$ of the $n-$th electron shell of the sulfur ion. We denote with $\tilde{E}_n$ the energies of the calculated states of the $S^{3+}-H^+$ system and also the effective radius of the corresponding electron shell with $\tilde{R}_{S,n}$, where n is an eigenstate number. The nucleus charge of the sulfur atom is $(+16)$, while the nucleus charge of the ion is evidently S^{3+}. It is known that the energies of states are proportional to the ion charge, and the characteristic size of the electron cloud depends on the energy and ion charge approximately as the inverse square root. Therefore, $E_1 \approx \frac{16}{3}\tilde{E}_1 \approx 5.3\tilde{E}_1$ and $R_{S,1} \approx 0.43\tilde{R}_{S,1}$. Also, for the next energy level, we have estimates $E_2 \approx \frac{4}{9}E_1 \approx 2.4\tilde{E}_1$ and $R_{S,2} \approx 0.64\tilde{R}_{S,1}$. Finally, for the third, valence electron shell, $E_3 \approx \frac{9}{16}E_2 \approx 1.4\tilde{E}_1$ and $R_{S,3} \approx 0.86\tilde{R}_{S,1}$. That is, $R_{S,3} \approx \tilde{R}_{S,1}$ and the energies of valence electrons are close to the energy of the ground state of the $S^{3+} - H^+$ system. At the same time, the solution of the dynamic problem shows that the only explicitly participating electron is always at least at the 6th level of the $S^{3+} - H^+$ system, and its energy is always about 5 times greater than the energy of the valence electrons of S^{3+}. Thus, estimates show that there is a significant energy gap between the valence electrons of the sulfur ion and the explicitly calculated electron which corresponds to some spatial separation of the analysed particles. In this case, the approximation of the sulfur ion potential with the formula for the Coulomb potential may be somewhat rough, but for ion-atom collisions with energy of several eV, it is acceptable.

Another reason for the applicability of the Coulomb approximation for the S^{3+} potential is that the ions do not approach very closely during the collision. The H^+ is located as close as possible to the S^{3+} ion at a distance R of about $R_{min} = 2.5$ a.u. It is sufficient to allow the S^{3+} potential be approximated by the Coulomb potential.

6.2. Analysis of head-on collision simulation results

At the beginning of the process, the electron was represented by the 6th energy state, and it conserved this shape when the ions approached, although the energy values decreased for the ions close to each other. Therefore, it is natural that the electron kept the 6th energy state at the end, which means that no electron transfer was observed.

Further, we will discuss the next question. We know that the equations of classical and quantum mechanics are time-reversible. If the collision process were described only with the classical mechanics equations, then a head-on collision which unambiguously follows the process of scattering should exactly repeat the process of ions approaching, but in the opposite order.

Let us consider the solution $\Phi_n(\vec{r}, R(t))$ of equation (9), which depends on the distance $R(t)$ between the ions, which in turn depends on time. Since the electron is initially in the 6th energy state, we take $n = 6$. Let us substitute the function

$$\tilde{\Psi}(\vec{r}, t) = \exp\left(\int_0^t \frac{E_6(R(t'))}{i\hbar} dt'\right) \Phi_6(\vec{r}, R(t)) \tag{22}$$

into the non-stationary Schrödinger equation (6).

Below, we show that since ions move very slowly in comparison to electrons, the condition

$$\left|\hbar \frac{\partial}{\partial t} \Phi_6(\vec{r}, R(t))\right| \ll |E_6(R(t))\Phi_6(\vec{r}, R(t))| \tag{23}$$

is fulfilled. Indeed, let us denote as $\Phi_0(\vec{r})$ the stationary electron wavefunction of a resting hydrogen atom in the ground state. The electron wave function of a hydrogen atom moving with constant velocity $\vec{V}$ in the direction of the sulfur ion has the form $\Phi_{0,moving}(\vec{r}, t) = \Phi_0(\vec{r} - \vec{V}t - \vec{R_0})$, where $\vec{R_0}$ is the initial hydrogen ion position. We calculate the derivative $\frac{\partial \Phi_{0,moving}(\vec{r},t)}{\partial t} = -\nabla\Phi_0(\vec{r} - \vec{V}t - \vec{R_0}) * \vec{V}$. Then

$$\left|\frac{\partial \Phi_{0,moving}(\vec{r}, t)}{\partial t}\right| \leq \sup\left(|\nabla\Phi_0(\vec{r})|\right) |\vec{V}| \sim \frac{2A}{l}|\vec{V}|, \tag{24}$$

where A is the amplitude of the function $\Phi_0(\vec{r})$ and l is the electron cloud characteristic scale. Since in our considered system of particles, the initial electron cloud corresponds to the 6th state of the sulfur ion-hydrogen ion particle system, instead of $\Phi_0(\vec{r})$, we should write $\Phi_6(\vec{r})$. The estimate (24) is derived for the case where the colliding particles are far from each other. When the colliding particles approach each other, the electron cloud is divided into three parts, and we can assume that l decreases three times. However, the relative velocity of the particles also decrease. Since we are only interested in orders of magnitudes, we can also apply the estimate (24) directly to the collision process. For the right side (23) we have the estimate $\left|E_6(R(t))\tilde{\Psi}(\vec{r}, t)\right| \sim |E_6(R(t))|\, A$. Thus, the inequality (23) (taking into account that maximum $E_6(R(t)) \sim -22$ eV and $l = 1$ a.u.) converts to

$$\frac{2\hbar|\vec{V}|}{l|E_6(R(t))|} \sim 0.05 \ll 1. \tag{25}$$

Due to (25), the function $\tilde{\Psi}(\vec{r}, t)$ of (22) for the collision at very low, eV-range, energies satisfies the non-stationary Schrödinger equation (6) with high accuracy, and we can observe that the electron in the collision process is always in the 6th energy state, as at the beginning. One can also suggest the following explanation of why the electron of the H atom after a collision tends to remain with the H^+. It is known from the fundamentals of mechanics that when a particle of a very small mass interacts with particles of a very large mass, the energy of the light particle is conserved with high accuracy. More accurately, the energy of a light particle can change during interactions with heavy particles but it always approximately returns to its original value. The electron we explicitly take into account initially has some energy as the hydrogen atom, and this energy is quite large for the $S^{3+} - H^+$ ion system. Therefore, the

electron is located in a sufficiently high 6th excited energy state of the $S^{3+} - H^{+}$ ion system at the beginning. When the ions approach each other, as illustrated in the snapshots of Fig.1, a significant part of the electron cloud is not concentrated between the ions, but is in the vicinity of the ions and even outside the $S^{3+} - H^{+}$ ion pair. This is a consequence of the rather high energy of the electron. There are rather large gaps between the energy levels of the $S^{3+} - H^{+}$ ion system. Therefore, the mentioned property of approximate conservation of energy by a light particle can lead the electron to be inclined to return to the 6th energy state, which was the initial one. We see that, despite the rather large positive charge of the S^{3+} ion, it is not easy to transfer an electron from a hydrogen atom to a sulfur ion, as one might expect.

Finally, the function (22) and the estimation (23) are used not only to the head-on collision process but in general (as presented in the snapshots of Fig.1 and Fig.5). Such a regular course and outcome of the collision is explained by the large difference in the masses of the ions and the electron, and the significant energy of the electron in the H atom. Now let's analyze how one can transfer an electron to a sulfur ion as a result of particle head-on collision. First of all, for the process, the inequality (23) should be violated. This is possible at significant energies of colliding particles, for example in the keV range. The probability of transferring an electron greatly depends on the initial conditions of the collision. The absolute value of the expansion coefficients $\alpha_n(R)$ of

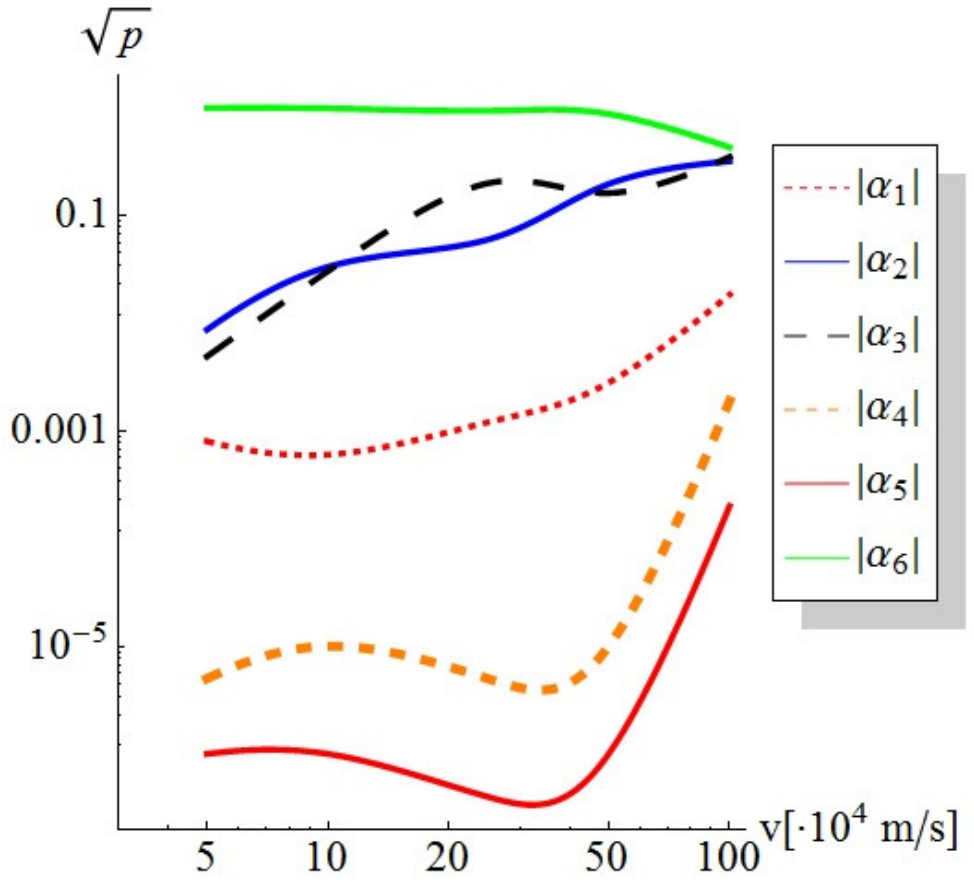

Figure 10. Velocity dependence of the absolute value of the expansion coefficients $\alpha_n(R)$ for $b = 0$ a.u. and the distance between ions $R = 10$ a.u. corresponding to five different energies E (13 eV, 52 eV, 325 eV, 1.3 keV and 5.2 keV).

the first six energy states for a head-on collision depending on the initial velocity of the hydrogen ion are presented in Fig.10. Table 3 and Table 4 present the absolute

Table 3. The absolute value of the expansion coefficients $\alpha_n(R)$ for $b = 2.5$ a.u. and the distance between ions $R = 8$ a.u. corresponding to five different energies E (13 eV, 52 eV, 325 eV, 1.3 keV and 5.2 keV).

$b = 2.5$ [a.u.]	$\lvert\alpha_1\rvert$	$\lvert\alpha_2\rvert$	$\lvert\alpha_3\rvert$	$\lvert\alpha_4\rvert$	$\lvert\alpha_5\rvert$	$\lvert\alpha_6\rvert$
$v = 5 \cdot 10^4$ [m/s]	$8 \cdot 10^{-4}$	$2.25 \cdot 10^{-2}$	$1.39 \cdot 10^{-2}$	$1.7 \cdot 10^{-3}$	$3 \cdot 10^{-6}$	0.9929
$v = 1 \cdot 10^5$ [m/s]	$8 \cdot 10^{-4}$	$1.44 \cdot 10^{-2}$	$1.6 \cdot 10^{-3}$	$4.6 \cdot 10^{-3}$	$3 \cdot 10^{-6}$	0.9921
$v = 2.5 \cdot 10^5$ [m/s]	$8 \cdot 10^{-4}$	$1.72 \cdot 10^{-2}$	$7.04 \cdot 10^{-2}$	$5.88 \cdot 10^{-2}$	$9 \cdot 10^{-6}$	0.9779
$v = 5 \cdot 10^5$ [m/s]	$9 \cdot 10^{-4}$	0.1248	0.1683	0.1129	$2 \cdot 10^{-5}$	0.8704
$v = 1 \cdot 10^6$ [m/s]	$8 \cdot 10^{-4}$	$5.12 \cdot 10^{-2}$	0.3672	0.1527	$3 \cdot 10^{-5}$	0.4806

Table 4. The absolute value of the expansion coefficients $\alpha_n(R)$ for $b = 5.0$ a.u. and the distance between ions $R = 9$ a.u. corresponding to five different energies E (13 eV, 52 eV, 325 eV, 1.3 keV and 5.2 keV).

$b = 5.0$ [a.u.]	$\lvert\alpha_1\rvert$	$\lvert\alpha_2\rvert$	$\lvert\alpha_3\rvert$	$\lvert\alpha_4\rvert$	$\lvert\alpha_5\rvert$	$\lvert\alpha_6\rvert$
$v = 5 \cdot 10^4$ [m/s]	$7 \cdot 10^{-4}$	$4.8 \cdot 10^{-3}$	$9 \cdot 10^{-4}$	$1.7 \cdot 10^{-3}$	$7 \cdot 10^{-7}$	0.9958
$v = 1 \cdot 10^5$ [m/s]	$8 \cdot 10^{-4}$	$5.9 \cdot 10^{-3}$	$7 \cdot 10^{-4}$	$1.1 \cdot 10^{-3}$	$6 \cdot 10^{-7}$	0.9942
$v = 2.5 \cdot 10^5$ [m/s]	$8 \cdot 10^{-4}$	$5.3 \cdot 10^{-3}$	$1.2 \cdot 10^{-3}$	$2.5 \cdot 10^{-3}$	$4 \cdot 10^{-7}$	0.9853
$v = 5 \cdot 10^5$ [m/s]	$8 \cdot 10^{-4}$	$1.3 \cdot 10^{-3}$	$4.54 \cdot 10^{-2}$	$4.3 \cdot 10^{-2}$	$2 \cdot 10^{-6}$	0.914
$v = 1 \cdot 10^6$ [m/s]	$8 \cdot 10^{-4}$	$8.31 \cdot 10^{-2}$	0.1076	$6.01 \cdot 10^{-2}$	$2 \cdot 10^{-6}$	0.791

values of the expansion coefficients $\alpha_n(R)$ corresponding to the impact parameters b equal to 2.5 a.u. and 5.0 a.u.

The calculation results for a collision energy of $E = 5$ keV showed that it is highly probable that an electron is transferred from the hydrogen atom to the sulfur ion and the single electron transfer may occur. For the range of collision energies of several hundred eVs, the transfer probability of an electron from hydrogen to the sulfur ion is lower (and it takes place more likely in a head-on collision). We should also note that at very high collision energies, the valence electron shell of the sulfur ion may be destroyed, and the process becomes generally very complex. We should also note that during the collision, the electron cloud changes significantly and rapidly. This can lead to the emission of electromagnetic waves. The radiation can facilitate the transition of the electron to the sulfur ion because the electron can lose part of its energy to the radiation. The energy loss is favourable for the transition of the electron to the sulfur ion. However, such a discussion is beyond the scope of this work.

7. Conclusions

In this paper, the problem of an atom-ion collision is considered using a simple model of a hydrogen atom with an S^{3+} ion and numerical calculations. The system of considered particles consisted of two positive ions and one electron. The valence electrons of the sulfur ion were not counted as individual particles.

Of course, such a simple model of the sulfur ion somewhat coarsens the description, but the model's simplicity is an important advantage of our approach since it is possible to carry out all further simulations and study the general scheme of the process.

The dynamics of the ions are described with the classical mechanics equations, while the electron dynamics is described with the Schrödinger equation. The classical description of the ions is justified by the fact that the scattering cross-sections of the colliding particles were not calculated, but only the charge transfer during a collision. In such a description, the problem under consideration is close to the semiclassical

in molecular physics at low velocities, where the positions of the nuclei are fixed and are described classically. To analyze solutions to the dynamic problem, the first six eigenstates of the $S^{3+} - H^{+}$ system were calculated, which depend on the distance R between the ions. To calculate the eigenstates, the proposed version of the FDM was used and the finite-difference technique, which makes the representation of eigenstates compatible with the representation of a solution to the collision dynamics problem. FDMs-based calculations are attractive because they do not require a set of basis functions to approximate the solution (as it is in the case of quantum chemistry packages), and the difficult question of whether the small set of basis functions used in the calculations is sufficient does not arise. The accuracy of the calculations is easier to control. The precision of the solution is influenced by the choice of appropriate initial and boundary conditions which must accurately represent the physical system. The sum of the squares of the expansion coefficients was also calculated and, for the collision at very low eV-range energies, it is always close to 1. Moreover, the absolute values of the first five expansion coefficients were always less than $6 \cdot 10^{-2}$, which means that these energy states practically did not participate in the collision. The performed simulations of head-on collision showed that the electron returns to the H ion after the collision. This can be explained as follows: the electron is always in the collision process in the same initial electronic state, however, it changes significantly during the collision and it is taking into account that the collision energies are not very high. Although, at sufficiently high collision energies, when the proposed estimate (25) is not preserved, it is highly probable that for the collision at the keV energy range an electron after the collision will be transferred from the hydrogen atom to the sulfur ion. Furthermore, studying the collision between S^{3+} and H with specified impact parameters for different ranges of the energies (from eVs to keVs) involved considering both classical and quantum mechanical aspects. Results obtained from our calculations show that the impact parameter choice influences the trajectories of the colliding particles, and the resulting scattering patterns provide valuable information about the ion-atom interaction. Insights gained from these simulations contribute also to a deeper understanding and interpretation of the collision dynamics.

In summary, a mixed quantum-classical description of ion-atom dynamics applied here provides a valuable compromise between the detailed quantum mechanical treatment and the computational efficiency of classical mechanics making it suitable for studying large and complex systems. The method proposed is versatile and can be adapted to different collision scenarios and environmental conditions, making it a valuable tool for studying a wide range of ion-atom interactions.

Acknowledgements

This work was performed in the framework of the cooperation between Immanuel Kant Baltic Federal University and Gdańsk University of Technology. The authors thank Sergey Leble for his attention to this work, complementary discussions, and consultations. We thank the Erasmus Plus Programme (M.Ł.and S. K.) for financial support. We acknowledge the allocation of computer time at the Academic Computer Centre in Gdańsk (CI TASK) and Wroclaw Centre for the Supercomputing (WCSS).

References

[1] B. H. Brandsen and M. R. C, McDowell, *Charge Exchange and the Theory of Ion-Atom Collisions*, (Oxford University Press, Oxford, 1992).

[2] D. R. Bates, *Atomic and Molecular Processes*, (Academic Press, New York, U.S., 1962).

[3] M. R. McDowell and J. P. Coleman, *Introduction to the Theory of Ion-Atom Collisions*, (Elsevier Science Publishing Co Inc., Amsterdam-London, 1970).

[4] Y. Ng, T. Baer, I. Powis, In Wiley Series in Ion Chemistry and Physics, *Unimolecular And Biomolecular Ion-molecule Reaction Dynamics*, (John Wiley and Sons, New York, U.S., 1994).

[5] G. A. Shields, A. Dalgarno and A. Sternberg, *Line emission from charge transfer with atomic hydrogen at thermal energies*, Phys. Rev. A **28**, 2137, 1983.

[6] J. Kingdon and G. Ferland, *The Effects of Charge Transfer on the Thermal Equilibrium of Photoionized Nebulae*, Astrophys. J. **516**, L107 (1999).

[7] Y. C. Ng, In Techniques of Chemistry Eds, J. N. Farrar and W. H. Saunders, *Techniques for the Study of Ion-Molecule Reactions*, (John Wiley and Sons Inc., U.K., 1988).

[8] M. C. Bacchus-Montabonel, M. Łabuda, Y. S. Tergiman, J. E. Sienkiewicz, *Theoretical treatment of charge-transfer processes induced by collision of Cq+ ions with uracil* Phys. Rev. A **72**, 052706 (2005).

[9] C. C. Havener, M. S. Huq, H. F. Krause, P. A. Schulz, and R. A. Phaneuf, *Merged-beams measurements of electron-capture cross sections for O5+ +H at electron-volt energies*, Phys. Rev. A **39**, 1725 (1989).

[10] A. K. Belyaev, J. Grosser, J. Hahne, and T. Menzel, *Ab initio cross sections for low-energy inelastic H+Na collisions*, Phys. Rev. A **60**, 2151 (1999).

[11] M. S. Pindzola, F. Robicheaux, S. D. Loch, J. C. Berengut, T. Topcu, J. Colgan, M. Foster, D. C. Griffin, C. P. Ballance, D. R. Schultz, T. Minami, N. R. Badnell, M. C. Witthoeft, D. R. Plante, D. M. Mitnik, J. A. Ludlow, U. Kleiman, *The time-dependent close-coupling method for atomic and molecular collision processes*, J. Phys. B: At. Mol. Opt. Phys. **40**, R39 (2007).

[12] M. Łabuda, Y. S. Tergiman, M. C. Bacchus-Montabonel, J. E. Sienkiewicz, *Ab initio molecular treatment for charge transfer by S3+ ion on hydrogen*, Chem. Phys. Lett., **394**, 446, (2004).

[13] R. E. Wyatt and J. Z. H. Zhang, *Dynamics of Molecules and Chemical Reactions*, (Marcel Dekker Inc., New York, 1996).

[14] M. Gargaud, M. C. Bacchus-Montabonel and R. McCarroll, *Charge transfer of O2+ in helium at thermal and low electron volt energies*, J. Chem. Phys. **99**, 449 (1993).

[15] R. G. Newton, *Scattering Theory of Waves and Particles*, (Springer Verlag, Berlin, Germany, 1982).

[16] D. G. Truhlar and J. T. Muckerman, *Reactive Scattering Cross Sections: Quasiclassical and Semiclassical Methods* in Atom-Molecule Collision Theory: A Guide for the Experimentalist, edited by R. B. Bernstein (Plenum Press, New York, 1979).

[17] D. Babikov, F. Aguillon, M. Sizun and V. Sidis, *Fragmentation of Na_2^+ dimer ions in kilo-electron-volt collisions with He: A coupled wave-packet study*, Phys. Rev. A **59**, 330-341 (1999).

[18] E. Balöitcha, M. Desouter-Lecomte, M. C. Bacchus-Montabonel, N. J. Vaeck, *Wave packet methods for charge exchange processes in ion-atom collisions*, J. Chem. Phys. **114**, 874 (2001).

[19] C. Leforestier and W. H. Miller, *Quantum mechanical calculation of the rate constant for the reaction H+O2?OH+O*, J. Chem. Phys. **100**, 733 (1994).

[20] D. Tannor, *Introduction to quantum mechanics, A time-dependent perspective*, (University Science Books, Sausalito, California, 2007).

[21] H. J. Eom, *Wave Scattering Theory*, (Springer-Verlag Berlin and Heidelberg GmbH & Co, Heidelberg, 2011).

[22] M. Łabuda, J. González-Vázquez, L. González, *A wavepacket study of the low-energy*

charge transfer process in the $S^{3+} + H$ reaction using time-resolved electronic densities, Phys. Chem. Chem.Phys. **12**, 5439 (2010).
[23] M. Łabuda, J. González-Vázquez, F. Martin, L. González, *A non-adiabatic wavepacket dynamical study of the low energy charge transfer process in the $S^{3+}+H$ collision*, Chemical Physics **400**, 165 (2012).
[24] A. de la Lande, B. Lévy, and I. Demachy, in *Reaction Rate Constant Computations: Theories and Applications*, ed. K. Han and T. Chu, (The Royal Society of Chemistry, Cambridge, 2013) pp. 99-132.
[25] D. Bostan, B. Mandal, C. Joy and D. Babikov, *Description of quantum interference using mixed quantum/classical theory of inelastic scattering*, Physical Chemistry Chemical Physics **25**, 15683, (2023).
[26] B. Mandal, C. Joy, D. Bostan, A. Eng, and D. Babikov, *Adiabatic Trajectory Approximation: A New General Method in the Toolbox of Mixed Quantum/Classical Theory for Collisional Energy Transfer*, The Journal of Physical Chemistry Letters **14**, 817-824 (2023).
[27] B. Mandal, C. Joy, A. Semenov, and D. Babikov, *Mixed Quantum/Classical Theory for Collisional Quenching of PAHs in the Interstellar Media* ACS Earth and Space Chemistry **6** 521-529 (2022).
[28] G. J. Ferland, K. T. Korista, D. A. Verner, J. W. Ferguson, J. B. Kingdon and E. M. Verner, *CLOUDY 90: Numerical Simulation of Plasmas and Their Spectra*, Publications of the Astronomical Society of the Pacific **110**, 761 (1998).
[29] G. Shen, P. C. Stancil, J. G. Wang, J. F. McCann and B. M. McLaughlin, *Radiative charge transfer in cold and ultracold sulphur atoms colliding with protons*, J. Phys. B: At. Mol. Opt. Phys. **48**, 105203 (2015).
[30] N. P. Abel, S. R. Federman, and P. C. Stancil, *The Effects of Doubly Ionized Chemistry on SH+ and S+2 Abundances in X-Ray-dominated Regions*, The Astrophysical Journal, **675**, L81–L84, (2008).
[31] D. Bostan et al., *Mixed quantum/classical calculations of rotationally inelastic scattering in the CO + CO system: a comparison with fully quantum results* Physical Chemistry Chemical Physics **26**, 6627, (2024).
[32] A. Horsfield et al. *Beyond Ehrenfest: correlated non-adiabatic molecular dynamics*, J. Phys.: Condens. Matter **16**, 8251 (2004).
[33] A. Kirrander and M. Vacher *Ehrenfest Methods for Electron and Nuclear Dynamics.* in Quantum Chemistry and Dynamics of Excited States: Methods and Applications (eds L. González and R. Lindh), (John Wiley & Sons, Inc, Hoboken, New Yersey,2020) Chapter 15. https://doi.org/10.1002/9781119417774.ch15
[34] I. Wayan Sudiarta and D. J. Wallace Geldart, *Solving the Schrödinger equation using the finite difference time domain method*, J. Phys. A: Math. Theor. **40**, 1885 (2007).
[35] M. Horbatsch, *Numerical solution of the time-dependent Schrödinger equation for monopole polarisation in ion-atom collisions*, J. Phys. B: At. Mol. Phys. **17**, 2591 (1984).
[36] S. Kshevetskii, The Conference Material of X International Workshop: Waves in Heterogeneous Media and Integrable Systems, Vol. 86 (Immanuel Kant Baltic Federal University (IKBFU), Kaliningrad, 2020).
[37] R. Richtmyer, *Principles of advanced mathematical physics*, (Springer-Verlag, New York, U.S., 1998).
[38] A. N. Tikhonov and A. A. Samarskii, *Equations of Mathematical Physics*, (Dover Publications, New York, 1990).
[39] G. B. Arkfen and H. J. Weber, *Mathematical Methods for Physicists*, (Harcourt, San Diego, U.S., 2001).